

## Investigating dynamic stability of metal foam nanoplates under periodic in-plane loads via a three-unknown plate theory

Raad M. Fenjan, Ridha A. Ahmed and Nadhim M. Faleh\*

*Al-Mustansiriah University, Engineering Collage P.O. Box 46049, Bab-Muadum, Baghdad 10001, Iraq*

*(Received December 18, 2018, Revised February 21, 2019, Accepted February 22, 2019)*

**Abstract.** Dynamic stability of a porous metal foam nano-dimension plate on elastic substrate exposed to bi-axial time-dependent forces has been studied via a novel 3-variable plate theory. Various pore contents based on uniform and non-uniform models have been introduced. The presented plate model contains smaller number of field variables with shear deformation verification. Hamilton's principle will be utilized to deduce the governing equations. Next, the equations have been defined in the context of Mathieu-Hill equation. Correctness of presented methodology has been verified by comparison of derived results with previous data. Impacts of static and dynamical force coefficients, non-local coefficient, foundation coefficients, pore distributions and boundary edges on stability regions of metal foam nanoscale plates will be studied.

**Keywords:** dynamic stability; 3-unknown plate theory; porous nanoplate; non-local elasticity; porosities

### 1. Introduction

Lightweight materials have been extensively utilized in multitude engineering fields owing to possessing desirable toughness comparing to their weights. A porous material, for instance a steel foam, might be placed in the category of lightweight materials and can be applied in several structures such as sandwich panels. Often, pore variation along the thickness of panels/plates results in a notable alteration in every kind of material property. Thus, such pore-dependent material might be the main topic of research for researchers or engineers. The most important examples are the works done by Jabbari *et al.* (2014), Chen *et al.* (2015, 2016), Rezaei and Saidi (2016) on metal foam structures.

When the pore distribution inside the material is selected to be non-uniform, the metal foam might be defined as a functionally graded material since its properties obey some specified functions. However, the term functionally graded is not used only for non-uniform porous metal foams only. This term is a general term for a variety of materials in which the properties are graded and are not uniform. One example is a functionally graded (FG) material based on two components which are ceramic and metal. In fact, the properties are graded from ceramic to metal. In such gradation of material properties, porosities could be inevitable (Wattanasakulpong *et al.* 2014). Due to contribution of two materials in this FG material, porosities occur as a sequence of material combination defect. Many researches have been focused on such FG material based

---

\*Corresponding author, Professor, E-mail: [dr.nadhim@uomustansiriyah.edu.iq](mailto:dr.nadhim@uomustansiriyah.edu.iq)

structures with the consideration of pore effect (Yahia *et al.* 2015, Atmane *et al.* 2015a, b, Barati and Zenkour 2016, Mechab *et al.* 2016, Mirjavadi *et al.* 2018, 2019a, b).

A structure at nano scale could not be modeled based on well-known elasticity theory which is used for macro size structures. This shortcoming comes from the inexistence of a scale parameter in classical elasticity. Thus, non-classical or higher order elasticity theories will be utilized in order to mathematically model a structure a nano scale. Such mathematical modeling is of great importance since experiments at nano level are still difficult. As a consequence, the well-known non-local elasticity (Eringen 1983) is notably used in such mathematical modeling for structures at nano level. After this mathematical modeling, it is possible to analyze structural behaviors of beams, plates and shell having nano-dimension. Some examples are the works done by Ebrahimi and Heidari (2018), Natarajan *et al.* (2012), Bounouara *et al.* (2016), Barati *et al.* (2016), Belkorissat *et al.* (2015), Barati (2017a, b), Zenkour (2016), Ebrahimi and Daman (2016), Mirjavadi *et al.* (2018), Ebrahimi and Haghgi (2018), and Ebrahimi *et al.* (2018).

In this research, a thick plate model is studied based on 3 field variables (Houari *et al.* 2016, Belabed *et al.* 2018). Note that classical plate model doesn't consider shear deformations for thick plates (Zenkour 2009, Mehala *et al.* 2018, Sadoun *et al.* 2018, Mahmoudi *et al.* 2018). Based on introduced plate theory, dynamic instability of nano-scale plates made of metal foam exposed to in-plane periodic loads will be studied. The material is steel with different pore distributions inside it. Nonlocal effects due to nano-dimension of the plate have been considered. The governing equations of the nano-dimension plate will be solved with the help of Galerkin's approach. The obtained stability regions due to applied periodic loads will be verified with the article of Han *et al.* 2015. The dynamic stability of metal foam nano-size plate is shown to be dependent on applied load factors, pore distribution, non-local impacts, and some other parameters.

## 2. Governing equations

### 2.1 Modeling of porous nanoplates

A porous material, for instance a steel foam, might be placed in the category of lightweight materials and can be applied in several structures such as sandwich panels. Often, pore variation along the thickness of panels/plates results in a notable alteration in every kind of material property. When the pore distribution inside the material is selected to be non-uniform, the metal foam might be defined as a functionally graded material since its properties obey some specified functions. Herein, the following types of pore dispersion will be employed:

- Uniform kind

$$E = E_2(1 - e_0\chi) \quad (1a)$$

$$G = G_2(1 - e_0\chi) \quad (1b)$$

$$\rho = \rho_2\sqrt{1 - e_0\chi} \quad (1c)$$

- Non-uniform kind 1

$$E(z) = E_2\left(1 - e_0 \cos\left(\frac{\pi z}{h}\right)\right) \quad (2a)$$

$$G(z) = G_2(1 - e_0 \cos\left(\frac{\pi z}{h}\right)) \tag{2b}$$

$$\rho(z) = \rho_2(1 - e_m \cos\left(\frac{\pi z}{h}\right)) \tag{2c}$$

• Non-uniform kind 2

$$E(z) = E_2(1 - e_0 \cos\left(\frac{\pi z}{2h} + \frac{\pi}{4}\right)) \tag{3a}$$

$$G(z) = G_2(1 - e_0 \cos\left(\frac{\pi z}{2h} + \frac{\pi}{4}\right)) \tag{3b}$$

$$\rho(z) = \rho_2(1 - e_m \cos\left(\frac{\pi z}{2h} + \frac{\pi}{4}\right)) \tag{3c}$$

The most important factors in above relations are the greatest values of material properties  $E_2$ ,  $G_2$  and  $\rho_2$ . Also, there are two important factors related to pores and mass which are  $e_0$  and  $e_m$  as

$$e_0 = 1 - \frac{E_2}{E_1} = 1 - \frac{G_2}{G_1} \tag{4a}$$

$$e_m = 1 - \frac{\rho_2}{\rho_1} \tag{4b}$$

Based on the open cell assumption of porous material, we use the following relations

$$\frac{E_2}{E_1} = \left(\frac{\rho_2}{\rho_1}\right)^2 \tag{5}$$

$$e_m = 1 - \sqrt{1 - e_0} \tag{6}$$

Based on uniformly distributed pores, the following parameter is used in Eq.(1) as

$$\chi = \frac{1}{e_0} - \frac{1}{e_0} \left( \frac{2}{\pi} \sqrt{1 - e_0} - \frac{2}{\pi} + 1 \right)^2 \tag{7}$$

Modeling of the nanoplate is performed employing a 3-unknown plate theory which has fewer field unknowns compared with the refined 4-unknown and also first order plate theory. The displacement fields of 3-unknown plate model can be expressed as

$$d_1(x, y, z, t) = u(x, y) - z \frac{\partial w}{\partial x} - \Theta(z) \frac{\partial^3 w}{\partial x^3} \tag{8a}$$

$$d_2(x, y, z, t) = v(x, y) - z \frac{\partial w}{\partial y} - \Theta(z) \frac{\partial^3 w}{\partial y^3} \quad (8b)$$

$$d_3(x, y, z, t) = w(x, y) \quad (8c)$$

Here,  $u$ ,  $v$  and  $w$  are field variables; actually  $w$  is the deflection. For better modeling of FG structures, it is crucial to consider the exact positions of neutral surface. Generally, there is coupling among membrane and lateral displacements of FGM plates, as it can be seen in Eqs.(8a) and (8b). By considering the concept of neutral surface, it is possible to eliminate this coupling. So, the displacement field of 3-unknown plate model can be reduced to the following form

$$d_1(x, y, z, t) = -(z - z^*) \frac{\partial w}{\partial x} - (\Theta(z) - z^{**}) \frac{\partial^3 w}{\partial x^3} \quad (9a)$$

$$d_2(x, y, z, t) = -(z - z^*) \frac{\partial w}{\partial y} - (\Theta(z) - z^{**}) \frac{\partial^3 w}{\partial y^3} \quad (9b)$$

$$d_3(x, y, z, t) = w(x, y, t) \quad (9c)$$

This is evident that the displacement field is reduced to a single-unknown model and

$$z^* = \frac{\int_{-h/2}^{h/2} E(z) z dz}{\int_{-h/2}^{h/2} E(z) dz}, \quad z^{**} = \frac{\int_{-h/2}^{h/2} E(z) \Theta(z) dz}{\int_{-h/2}^{h/2} E(z) dz} \quad (10)$$

In above relations, the function  $\Theta$  will be defined as

$$\Theta(z) = \cosh\left(\frac{\pi}{2}\right) \frac{h^3}{2\pi^2} \sin\left(\frac{\pi z}{h}\right) \quad (11)$$

Finally, the strains based on the four-unknown plate model are obtained as

$$\begin{Bmatrix} \varepsilon_x \\ \varepsilon_y \\ \gamma_{xy} \end{Bmatrix} = \begin{Bmatrix} \varepsilon_x^0 \\ \varepsilon_y^0 \\ \gamma_{xy}^0 \end{Bmatrix} + z \begin{Bmatrix} \kappa_x \\ \kappa_y \\ \kappa_{xy} \end{Bmatrix} + \Theta(z) \begin{Bmatrix} \eta_x \\ \eta_y \\ \eta_{xy} \end{Bmatrix}, \quad \begin{Bmatrix} \gamma_{yz} \\ \gamma_{xz} \end{Bmatrix} = g(z) \begin{Bmatrix} \gamma_{yz} \\ \gamma_{xz} \end{Bmatrix} \quad (12a)$$

where  $g(z) = \Theta'(z)$  and

$$\begin{Bmatrix} \varepsilon_x^0 \\ \varepsilon_y^0 \\ \gamma_{xy}^0 \end{Bmatrix} = \begin{Bmatrix} \frac{\partial u}{\partial x} \\ \frac{\partial v}{\partial y} \\ \frac{\partial u}{\partial y} + \frac{\partial v}{\partial x} \end{Bmatrix}, \quad \begin{Bmatrix} \kappa_x \\ \kappa_y \\ \kappa_{xy} \end{Bmatrix} = \begin{Bmatrix} -\frac{\partial^2 w}{\partial x^2} \\ -\frac{\partial^2 w}{\partial y^2} \\ -2\frac{\partial^2 w}{\partial x \partial y} \end{Bmatrix}, \quad \begin{Bmatrix} \eta_x \\ \eta_y \\ \eta_{xy} \end{Bmatrix} = \begin{Bmatrix} \frac{\partial^4 w}{\partial x^2} \\ \frac{\partial^4 w}{\partial y^2} \\ \frac{\partial^2 (\nabla^2 w)}{\partial x \partial y} \end{Bmatrix}, \quad \begin{Bmatrix} \gamma_{yz} \\ \gamma_{xz} \end{Bmatrix} = \begin{Bmatrix} \frac{\partial^3 w}{\partial y^3} \\ \frac{\partial^3 w}{\partial x^3} \end{Bmatrix} \quad (12b)$$

Next, one might express the Hamilton's rule as follows based on strain energy (U) and kinetic energy (T)

$$\int_0^t \delta(U - T + V) dt = 0 \tag{13}$$

and V is the work of non-conservative loads. Based on above relation we have

$$\delta U = \int_V \sigma_{kl} \delta \varepsilon_{kl} dV = \int_V (\sigma_x \delta \varepsilon_x + \sigma_y \delta \varepsilon_y + \sigma_{xy} \delta \gamma_{xy} + \sigma_{yz} \delta \gamma_{yz} + \sigma_{xz} \delta \gamma_{xz}) dV \tag{14a}$$

Inserting Eqs. (13) into Eq.(14a) lead to

$$\begin{aligned} \delta U = \int_0^a \int_0^b [N_x \delta \varepsilon_x^0 - M_x \delta \kappa_x - S_x \delta \eta_x + N_y \delta \varepsilon_y^0 - M_y \delta \kappa_y - S_y \delta \eta_y \\ + N_{xy} \delta \gamma_{xy}^0 - M_{xy} \delta \kappa_{xy} - S_{xy} \delta \eta_{xy} + Q_{yz} \delta \gamma_{yz} + Q_{xz} \delta \gamma_{xz}] dx dy \end{aligned} \tag{14b}$$

in which

$$\begin{aligned} (N_k, M_k^b, M_k^s) = \int_{-h/2}^{h/2} (1, z, \Theta) \sigma_k dz, \quad k = \{x, y, xy\} \\ Q_l = \int_{-h/2}^{h/2} g \sigma_l dz, \quad l = \{xz, yz\} \end{aligned} \tag{14c}$$

The variation of the work of non-conservative forces is expressed by

$$\delta V = \int_0^a \int_0^b (N_x^0 \frac{\partial w}{\partial x} \frac{\partial \delta w}{\partial x} + N_y^0 \frac{\partial w}{\partial y} \frac{\partial \delta w}{\partial y} + 2\delta N_{xy}^0 \frac{\partial w}{\partial x} \frac{\partial w}{\partial y} - k_w \delta w + k_p \frac{\partial^2 \delta w}{\partial x^2}) dy dx \tag{15}$$

where  $N_x^0, N_y^0, N_{xy}^0$  denote membrane forces and  $k_w, k_p$  are elastic substrate constants. Also, the kinetic energy variation is obtained as

$$\begin{aligned} \delta K = \int_0^a \int_0^b [I_0 (\frac{\partial u}{\partial t} \frac{\partial \delta u}{\partial t} + \frac{\partial v}{\partial t} \frac{\partial \delta v}{\partial t} + \frac{\partial w}{\partial t} \frac{\partial \delta w}{\partial t}) - I_1 (\frac{\partial u}{\partial t} \frac{\partial^2 \delta w}{\partial x \partial t} + \frac{\partial^2 w}{\partial x \partial t} \frac{\partial \delta u}{\partial t} + \frac{\partial v}{\partial t} \frac{\partial^2 \delta w}{\partial y \partial t} \\ + \frac{\partial^2 w}{\partial y \partial t} \frac{\partial \delta v}{\partial t}) - J_1 (\frac{\partial u}{\partial t} \frac{\partial^4 \delta w}{\partial x^3 \partial t} + \frac{\partial^4 w}{\partial x^3 \partial t} \frac{\partial \delta u}{\partial t} + \frac{\partial v}{\partial t} \frac{\partial^4 \delta w}{\partial y^3 \partial t} + \frac{\partial^4 w}{\partial y^3 \partial t} \frac{\partial \delta v}{\partial t}) + I_2 (\frac{\partial^2 w}{\partial x \partial t} \frac{\partial^2 \delta w}{\partial x \partial t} + \frac{\partial^2 w}{\partial y \partial t} \frac{\partial^2 \delta w}{\partial y \partial t}) \\ + K_2 (\frac{\partial^4 w}{\partial x^3 \partial t} \frac{\partial^4 \delta w}{\partial x^3 \partial t} + \frac{\partial^4 w}{\partial y^3 \partial t} \frac{\partial^4 \delta w}{\partial y^3 \partial t}) + J_2 (\frac{\partial^2 w}{\partial x \partial t} \frac{\partial^4 \delta w}{\partial x^3 \partial t} + \frac{\partial^4 w}{\partial x^3 \partial t} \frac{\partial^2 \delta w}{\partial x \partial t} + \frac{\partial^2 w}{\partial y \partial t} \frac{\partial^4 \delta w}{\partial y^3 \partial t} + \frac{\partial^4 w}{\partial y^3 \partial t} \frac{\partial^2 \delta w}{\partial y \partial t})] dy dx \end{aligned} \tag{16}$$

where

$$(I_0, I_1, J_1, I_2, J_2, K_2) = \int_{-h/2}^{h/2} (1, z, f, z^2, zf, f^2) \rho(z) dz \tag{17}$$

Substituting Eqs.(14)-(17) into Eq.(12) then collecting the coefficients of  $\delta u, \delta v, \delta w$  results in three equations of motion

$$\frac{\partial N_x}{\partial x} + \frac{\partial N_{xy}}{\partial y} - I_0 \frac{\partial^2 u}{\partial t^2} + I_1 \frac{\partial^3 w}{\partial x \partial t^2} + J_1 \frac{\partial^5 w}{\partial x^3 \partial t^2} = 0 \tag{18}$$

$$\frac{\partial N_{xy}}{\partial x} + \frac{\partial N_y}{\partial y} - I_0 \frac{\partial^2 v}{\partial t^2} + I_1 \frac{\partial^3 w}{\partial y \partial t^2} + J_1 \frac{\partial^5 w}{\partial y^3 \partial t^2} = 0 \tag{19}$$

$$\begin{aligned}
& \frac{\partial^2 M_x}{\partial x^2} + 2 \frac{\partial^2 M_{xy}}{\partial x \partial y} + \frac{\partial^2 M_y}{\partial y^2} + \frac{\partial^4 S_x}{\partial x^4} + \frac{\partial^2 S_{xy}^4}{\partial x^3 \partial y} + \frac{\partial^2 S_{xy}^4}{\partial x \partial y^3} + \frac{\partial^4 S_y}{\partial y^4} - \frac{\partial^3 Q_{xz}}{\partial x^3} - \frac{\partial^3 Q_{yz}}{\partial y^3} \\
& -k_w w - k_p \nabla^2 w - N_0 \nabla^2 w = I_0 \frac{\partial^2 w}{\partial t^2} + I_1 \left( \frac{\partial^3 u}{\partial x \partial t^2} + \frac{\partial^3 v}{\partial y \partial t^2} \right) + J_1 \left( \frac{\partial^5 u}{\partial x^3 \partial t^2} + \frac{\partial^5 v}{\partial y^3 \partial t^2} \right) \\
& -I_2 \left( \frac{\partial^4 w}{\partial x^2 \partial t^2} + \frac{\partial^4 w}{\partial y^2 \partial t^2} \right) - 2J_2 \left( \frac{\partial^6 w}{\partial x^4 \partial t^2} + \frac{\partial^6 w}{\partial y^4 \partial t^2} \right) - K_2 \left( \frac{\partial^8 w}{\partial x^6 \partial t^2} + \frac{\partial^8 w}{\partial y^6 \partial t^2} \right)
\end{aligned} \quad (20)$$

Based on nonlocal elasticity theory, the nonlocality of stress field can be incorporated into the stress-strain relationship as

$$(1 - (e_0 a) \nabla^2) \sigma_{kl} = t_{kl} \quad (21)$$

in which  $\nabla^2$  denotes the Laplacian parameter and  $e_0 a$  is a scale parameter introducing the small size impact. Finally, the nonlocal constitutive relations based on refined FG plate model can be expressed by

$$(1 - \mu \nabla^2) \begin{Bmatrix} \sigma_x \\ \sigma_y \\ \sigma_{xy} \\ \sigma_{yz} \\ \sigma_{xz} \end{Bmatrix} = \begin{pmatrix} Q_{11} & Q_{12} & 0 & 0 & 0 \\ Q_{12} & Q_{22} & 0 & 0 & 0 \\ 0 & 0 & Q_{66} & 0 & 0 \\ 0 & 0 & 0 & Q_{44} & 0 \\ 0 & 0 & 0 & 0 & Q_{55} \end{pmatrix} \begin{Bmatrix} \varepsilon_x \\ \varepsilon_y \\ \gamma_{xy} \\ \gamma_{yz} \\ \gamma_{xz} \end{Bmatrix} \quad (22)$$

where

$$Q_{11} = Q_{22} = \frac{E(z)}{1 - \nu^2(z)}, \quad Q_{12} = \nu(z) Q_{11}, \quad Q_{44} = Q_{55} = Q_{66} = \frac{E(z)}{2(1 + \nu(z))} \quad (23)$$

After integrating Eq. (23) in thickness direction, we get to the following relationships

$$(1 - \mu \nabla^2) \begin{Bmatrix} N_x \\ N_y \\ N_{xy} \end{Bmatrix} = \begin{pmatrix} A_{11} & A_{12} & 0 \\ A_{12} & A_{22} & 0 \\ 0 & 0 & A_{66} \end{pmatrix} \begin{Bmatrix} \frac{\partial u}{\partial x} \\ \frac{\partial v}{\partial y} \\ \frac{\partial u}{\partial y} + \frac{\partial v}{\partial x} \end{Bmatrix} + \begin{pmatrix} B_{11} & B_{12} & 0 \\ B_{12} & B_{22} & 0 \\ 0 & 0 & B_{66} \end{pmatrix} \begin{Bmatrix} \frac{\partial^2 w}{\partial x^2} \\ \frac{\partial^2 w}{\partial y^2} \\ -2 \frac{\partial^2 w}{\partial x \partial y} \end{Bmatrix} + \begin{pmatrix} B_{11}^s & B_{12}^s & 0 \\ B_{12}^s & B_{22}^s & 0 \\ 0 & 0 & B_{66}^s \end{pmatrix} \begin{Bmatrix} \frac{\partial^4 w}{\partial x^4} \\ \frac{\partial^4 w}{\partial y^4} \\ \frac{\partial^2 (\nabla^2 w)}{\partial x \partial y} \end{Bmatrix} \quad (24)$$

$$(1 - \mu \nabla^2) \begin{Bmatrix} M_x \\ M_y \\ M_{xy} \end{Bmatrix} = \begin{pmatrix} B_{11} & B_{12} & 0 \\ B_{12} & B_{22} & 0 \\ 0 & 0 & B_{66} \end{pmatrix} \begin{Bmatrix} \frac{\partial u}{\partial x} \\ \frac{\partial v}{\partial y} \\ \frac{\partial u}{\partial y} + \frac{\partial v}{\partial x} \end{Bmatrix} + \begin{pmatrix} D_{11} & D_{12} & 0 \\ D_{12} & D_{22} & 0 \\ 0 & 0 & D_{66} \end{pmatrix} \begin{Bmatrix} \frac{\partial^2 w}{\partial x^2} \\ \frac{\partial^2 w}{\partial y^2} \\ -2 \frac{\partial^2 w}{\partial x \partial y} \end{Bmatrix} + \begin{pmatrix} D_{11}^s & D_{12}^s & 0 \\ D_{12}^s & D_{22}^s & 0 \\ 0 & 0 & D_{66}^s \end{pmatrix} \begin{Bmatrix} \frac{\partial^4 w}{\partial x^4} \\ \frac{\partial^4 w}{\partial y^4} \\ \frac{\partial^2 (\nabla^2 w)}{\partial x \partial y} \end{Bmatrix} \quad (25)$$

$$(1 - \mu \nabla^2) \begin{Bmatrix} S_x \\ S_y \\ S_{xy} \end{Bmatrix} = \begin{pmatrix} B_{11}^s & B_{12}^s & 0 \\ B_{12}^s & B_{22}^s & 0 \\ 0 & 0 & B_{66}^s \end{pmatrix} \begin{Bmatrix} \frac{\partial u}{\partial x} \\ \frac{\partial v}{\partial y} \\ \frac{\partial u}{\partial y} + \frac{\partial v}{\partial x} \end{Bmatrix} + \begin{pmatrix} D_{11}^s & D_{12}^s & 0 \\ D_{12}^s & D_{22}^s & 0 \\ 0 & 0 & D_{66}^s \end{pmatrix} \begin{Bmatrix} \frac{\partial^2 w}{\partial x^2} \\ \frac{\partial^2 w}{\partial y^2} \\ -2 \frac{\partial^2 w}{\partial x \partial y} \end{Bmatrix} + \begin{pmatrix} H_{11}^s & H_{12}^s & 0 \\ H_{12}^s & H_{22}^s & 0 \\ 0 & 0 & H_{66}^s \end{pmatrix} \begin{Bmatrix} \frac{\partial^4 w}{\partial x^4} \\ \frac{\partial^4 w}{\partial y^4} \\ \frac{\partial^2 (\nabla^2 w)}{\partial x \partial y} \end{Bmatrix} \quad (26)$$

$$(1 - \mu \nabla^2) \begin{Bmatrix} Q_{xz} \\ Q_{yz} \end{Bmatrix} = \begin{pmatrix} A_{44}^s & 0 \\ 0 & A_{55}^s \end{pmatrix} \begin{Bmatrix} \frac{\partial^3 w}{\partial x^3} \\ \frac{\partial^3 w}{\partial y^3} \end{Bmatrix} \quad (27)$$

where

$$\begin{Bmatrix} A_{11}, B_{11}, B_{11}^s, D_{11}, D_{11}^s, H_{11}^s \\ A_{12}, B_{12}, B_{12}^s, D_{12}, D_{12}^s, H_{12}^s \\ A_{66}, B_{66}, B_{66}^s, D_{66}, D_{66}^s, H_{66}^s \end{Bmatrix} = \int_{-h/2}^{h/2} Q_{11}(1, z, \Theta, z^2, z\Theta, \Theta^2) \begin{Bmatrix} 1 \\ \nu \\ \frac{1-\nu}{2} \end{Bmatrix} dz \quad (28)$$

$$A_{44}^s = A_{55}^s = \int_{-h/2}^{h/2} g^2 \frac{E(z)}{2(1+\nu)} dz \quad (29)$$

Three equations of motion based on neutral surface location will be derived by placing Eqs. (25)-(28) into Eqs. (19)-(21) as follows

$$A_{11} \frac{\partial^2 u}{\partial x^2} + A_{66} \frac{\partial^2 u}{\partial y^2} + (A_{12} + A_{66}^s) \frac{\partial^2 v}{\partial x \partial y} - B_{11} \frac{\partial^3 w}{\partial x^3} - (B_{12} + 2B_{66}^s) \frac{\partial^3 w}{\partial x \partial y^2} - B_{11}^s \frac{\partial^5 w}{\partial x^5} - (B_{12}^s + B_{66}^s) \frac{\partial^5 w}{\partial x \partial y^4} - B_{66}^s \frac{\partial^5 w}{\partial x^3 \partial y^2} + (1 - \mu \nabla^2) (-I_0 \frac{\partial^2 u}{\partial t^2} + I_1 \frac{\partial^3 w}{\partial x \partial t^2} + J_1 \frac{\partial^5 w}{\partial x^3 \partial t^2}) = 0 \quad (30)$$

$$A_{66} \frac{\partial^2 v}{\partial x^2} + A_{22} \frac{\partial^2 v}{\partial y^2} + (A_{12} + A_{66}^s) \frac{\partial^2 u}{\partial x \partial y} - B_{22} \frac{\partial^3 w}{\partial y^3} - (B_{12} + 2B_{66}^s) \frac{\partial^3 w}{\partial x^2 \partial y} - B_{22}^s \frac{\partial^5 w}{\partial y^5} - (B_{12}^s + B_{66}^s) \frac{\partial^5 w}{\partial x^4 \partial y} - B_{66}^s \frac{\partial^5 w}{\partial x^2 \partial y^3} + (1 - \mu \nabla^2) (-I_0 \frac{\partial^2 v}{\partial t^2} + I_1 \frac{\partial^3 w}{\partial y \partial t^2} + J_1 \frac{\partial^5 w}{\partial y^3 \partial t^2}) = 0 \quad (31)$$

$$B_{11} \frac{\partial^3 u}{\partial x^3} + (B_{12} + 2B_{66}^s) \frac{\partial^3 u}{\partial x \partial y^2} + (B_{12} + 2B_{66}^s) \frac{\partial^3 v}{\partial x^2 \partial y} + B_{22} \frac{\partial^3 v}{\partial y^3} - D_{11} \frac{\partial^4 w}{\partial x^4} - 2(D_{12} + 2D_{66}^s) \frac{\partial^4 w}{\partial x^2 \partial y^2} - D_{22} \frac{\partial^4 w}{\partial y^4} + B_{11}^s \frac{\partial^5 u}{\partial x^5} + (B_{12}^s + B_{66}^s) \frac{\partial^5 u}{\partial x \partial y^4} + (B_{12}^s + B_{66}^s) \frac{\partial^5 v}{\partial x^4 \partial y} + B_{22}^s \frac{\partial^5 v}{\partial y^5} + B_{66}^s \frac{\partial^5 u}{\partial x^3 \partial y^2} + B_{66}^s \frac{\partial^5 v}{\partial x^2 \partial y^3} - 2D_{11}^s \frac{\partial^6 w}{\partial x^6} - 2(D_{12}^s + 2D_{66}^s) \frac{\partial^6 w}{\partial x^2 \partial y^4} - 2(D_{12}^s + 2D_{66}^s) \frac{\partial^6 w}{\partial x^4 \partial y^2} - 2D_{22}^s \frac{\partial^6 w}{\partial y^6} - H_{11}^s \frac{\partial^8 w}{\partial x^8} - 2(H_{12}^s + H_{66}^s) \frac{\partial^8 w}{\partial x^4 \partial y^4} - H_{66}^s \frac{\partial^8 w}{\partial x^6 \partial y^2} \quad (32)$$

$$\begin{aligned}
& -H_{66}^s \frac{\partial^8 w}{\partial x^2 \partial y^6} - H_{22}^s \frac{\partial^8 w}{\partial y^8} + A_{44}^s \frac{\partial^6 w}{\partial x^6} + A_{55}^s \frac{\partial^6 w}{\partial y^6} \\
& + (1 - \mu \nabla^2) \left( -I_0 \frac{\partial^2 w}{\partial t^2} - I_1 \left( \frac{\partial^3 u}{\partial x \partial t^2} + \frac{\partial^3 v}{\partial y \partial t^2} \right) - J_1 \left( \frac{\partial^5 u}{\partial x^3 \partial t^2} + \frac{\partial^5 v}{\partial y^3 \partial t^2} \right) \right) \\
& + I_2 \left( \frac{\partial^4 w}{\partial x^2 \partial t^2} + \frac{\partial^4 w}{\partial y^2 \partial t^2} \right) + 2J_2 \left( \frac{\partial^6 w}{\partial x^4 \partial t^2} + \frac{\partial^6 w}{\partial y^4 \partial t^2} \right) + K_2 \left( \frac{\partial^8 w}{\partial x^6 \partial t^2} + \frac{\partial^8 w}{\partial y^6 \partial t^2} \right) \\
& - N^0 \nabla^2 w - k_w w + k_p \nabla^2 w = 0
\end{aligned} \tag{32}$$

As mentioned, bending-extension coupling eliminates with consideration of neutral surface position. Three coupled governing equations might be reduced to a single equation in term of  $w$  by discarding  $u$  and  $v$  as

$$\begin{aligned}
& -\tilde{D}_{11} \frac{\partial^4 w}{\partial x^4} - 2(\tilde{D}_{12} + 2\tilde{D}_{66}) \frac{\partial^4 w}{\partial x^2 \partial y^2} - \tilde{D}_{22} \frac{\partial^4 w}{\partial y^4} - 2\tilde{D}_{11}^s \frac{\partial^6 w}{\partial x^6} - 2(\tilde{D}_{12}^s + 2\tilde{D}_{66}^s) \frac{\partial^6 w}{\partial x^2 \partial y^4} \\
& - 2(\tilde{D}_{12}^s + 2\tilde{D}_{66}^s) \frac{\partial^6 w}{\partial x^4 \partial y^2} - 2\tilde{D}_{22}^s \frac{\partial^6 w}{\partial y^6} - \tilde{H}_{11}^s \frac{\partial^8 w}{\partial x^8} - 2(\tilde{H}_{12}^s + \tilde{H}_{66}^s) \frac{\partial^8 w}{\partial x^4 \partial y^4} - \tilde{H}_{66}^s \frac{\partial^8 w}{\partial x^6 \partial y^2} \\
& - \tilde{H}_{66}^s \frac{\partial^8 w}{\partial x^2 \partial y^6} - \tilde{H}_{22}^s \frac{\partial^8 w}{\partial y^8} + \tilde{A}_{44}^s \frac{\partial^6 w}{\partial x^6} + \tilde{A}_{55}^s \frac{\partial^6 w}{\partial y^6} \\
& - \tilde{I}_0 \frac{\partial^2 w}{\partial t^2} + \mu \tilde{I}_0 \left( \frac{\partial^4 w}{\partial x^2 \partial t^2} \right) + \tilde{I}_2 \left( \frac{\partial^4 w}{\partial x^2 \partial t^2} + \frac{\partial^4 w}{\partial y^2 \partial t^2} \right) - \mu \tilde{I}_2 \left( \frac{\partial^6 w}{\partial x^4 \partial t^2} + 2 \frac{\partial^6 w}{\partial x^2 \partial y^2 \partial t^2} + \frac{\partial^6 w}{\partial y^4 \partial t^2} \right) \\
& + 2\tilde{J}_2 \left( \frac{\partial^6 w}{\partial x^4 \partial t^2} + \frac{\partial^6 w}{\partial y^4 \partial t^2} \right) - 2\mu \tilde{J}_2 \left( \frac{\partial^8 w}{\partial x^6 \partial t^2} + \frac{\partial^8 w}{\partial x^4 \partial y^2 \partial t^2} + \frac{\partial^8 w}{\partial x^2 \partial y^4 \partial t^2} + \frac{\partial^8 w}{\partial y^6 \partial t^2} \right) \\
& + \tilde{K}_2 \left( \frac{\partial^8 w}{\partial x^6 \partial t^2} + \frac{\partial^8 w}{\partial y^6 \partial t^2} \right) - \mu \tilde{K}_2 \left( \frac{\partial^{10} w}{\partial x^8 \partial t^2} + \frac{\partial^{10} w}{\partial x^6 \partial y^2 \partial t^2} + \frac{\partial^{10} w}{\partial x^2 \partial y^6 \partial t^2} + \frac{\partial^{10} w}{\partial y^8 \partial t^2} \right) \\
& - N^0 \left( \frac{\partial^2 w}{\partial x^2} + \frac{\partial^2 w}{\partial y^2} \right) + \mu N^0 \left( \frac{\partial^4 w}{\partial x^4} + 2 \frac{\partial^4 w}{\partial x^2 \partial y^2} + \frac{\partial^4 w}{\partial y^4} \right) - k_w w + \mu k_w \left( \frac{\partial^2 w}{\partial x^2} + \frac{\partial^2 w}{\partial y^2} \right) \\
& + k_p \left( \frac{\partial^2 w}{\partial x^2} + \frac{\partial^2 w}{\partial y^2} \right) - \mu k_p \left( \frac{\partial^4 w}{\partial x^4} + 2 \frac{\partial^4 w}{\partial x^2 \partial y^2} + \frac{\partial^4 w}{\partial y^4} \right) = 0
\end{aligned} \tag{33}$$

in which

$$\left\{ \begin{array}{l} \tilde{A}_{11}, \tilde{D}_{11}, \tilde{D}_{11}^s, \tilde{H}_{11}^s \\ \tilde{A}_{12}, \tilde{D}_{12}, \tilde{D}_{12}^s, \tilde{H}_{12}^s \\ \tilde{A}_{66}, \tilde{D}_{66}, \tilde{D}_{66}^s, \tilde{H}_{66}^s \end{array} \right\} = \int_{-h/2}^{h/2} Q_{11} (1, (z-z^*)^2, (z-z^*)(\Theta-z^{**}), (\Theta-z^{**})^2) \left\{ \begin{array}{l} 1 \\ \nu \\ \frac{1-\nu}{2} \end{array} \right\} dz \tag{34}$$

$$(\tilde{I}_0, \tilde{I}_2, \tilde{J}_2, \tilde{K}_2) = \int_{-h/2}^{h/2} (1, (z-z^*)^2, (z-z^*)(\Theta-z^{**}), (\Theta-z^{**})^2) \rho(z) dz \tag{35}$$

### 3. Solution procedure

The above single governing equation will be solved with the help of Galerkin's technique for a nano-dimension plate having bottom edge conditions:

Simply-supported (S):

$$w = \frac{\partial^2 w}{\partial x^2} = 0 \text{ at } x=0, a$$

$$w = \frac{\partial^2 w}{\partial y^2} = 0 \text{ at } y=0, b$$

Clamped (C):

$$w = \frac{\partial w}{\partial x} = 0 \text{ at } x=0, a \text{ and } y=0, b$$

Finally, the displacement field is considered as

$$w = \sum_{m=1}^{\infty} \sum_{n=1}^{\infty} W_{mn} F_m(x) F_n(y) e^{i\omega t} \tag{36}$$

where  $W_{mn}$  largest deflection. Placing Eq. (36) into Eq. (33) leads to

$$\begin{aligned} & -\tilde{D}_{11} \Lambda_{4000} - 2(\tilde{D}_{12} + 2\tilde{D}_{66}) \Lambda_{2200} - \tilde{D}_{22} \Lambda_{0400} - 2\tilde{D}_{11}^s \Lambda_{6000} - 2(\tilde{D}_{12}^s + 2\tilde{D}_{66}^s) \Lambda_{2400} \\ & - 2(\tilde{D}_{12}^s + 2\tilde{D}_{66}^s) \Lambda_{4200} - 2\tilde{D}_{22}^s \Lambda_{0600} - \tilde{H}_{11}^s \Lambda_{8000} - 2(\tilde{H}_{12}^s + \tilde{H}_{66}^s) \Lambda_{4400} - \tilde{H}_{66}^s \Lambda_{6200} \\ & - \tilde{H}_{66}^s \Lambda_{2600} - \tilde{H}_{22}^s \Lambda_{0800} + \tilde{A}_{44}^s \Lambda_{0600} + \tilde{A}_{55}^s \Lambda_{0600} \\ & - \omega^2 [-\tilde{I}_0 \Lambda_{0000} + \mu \tilde{I}_0 (\Lambda_{2000} + \Lambda_{0200}) + \tilde{I}_2 (\Lambda_{2000} + \Lambda_{0200}) - \mu \tilde{I}_2 (\Lambda_{4000} + 2\Lambda_{2200} + \Lambda_{0400}) \\ & + 2\tilde{J}_2 (\Lambda_{4000} + \Lambda_{0400}) - 2\mu \tilde{J}_2 (\Lambda_{6000} + \Lambda_{4200} + \Lambda_{2400} + \Lambda_{0600}) \\ & + \tilde{K}_2 (\Lambda_{6000} + \Lambda_{0600}) - \mu \tilde{K}_2 (\Lambda_{8000} + \Lambda_{6200} + \Lambda_{2600} + \Lambda_{0800}) \\ & - N^0 (\Lambda_{2000} + \Lambda_{0200}) + \mu N^0 (\Lambda_{4000} + 2\Lambda_{2200} + \Lambda_{0400}) - k_w \Lambda_{0000} + \mu k_w (\Lambda_{2000} + \Lambda_{0200}) \\ & + k_p (\Lambda_{2000} + \Lambda_{0200}) - \mu k_p (\Lambda_{4000} + 2\Lambda_{2200} + \Lambda_{0400})] = 0 \end{aligned} \tag{37}$$

where

$$\{\Lambda_{0000}, \Lambda_{2000}, \Lambda_{0200}\} = \int_0^a \int_0^b \{F_m(x) F_n(y), F_m^{(2)}(x) F_n(y), F_m(x) F_n^{(2)}(y)\} F_m(x) F_n(y) dx dy \tag{38}$$

$$\{\Lambda_{2200}, \Lambda_{4000}, \Lambda_{0400}\} = \int_0^a \int_0^b \{F_m^{(2)}(x) F_n^{(2)}(y), F_m^{(4)}(x) F_n(y), F_m(x) F_n^{(4)}(y)\} F_m(x) F_n(y) dx dy \tag{39}$$

$$\{\Lambda_{4400}, \Lambda_{6000}, \Lambda_{0600}\} = \int_0^a \int_0^b \{F_m^{(4)}(x) F_n^{(4)}(y), F_m^{(6)}(x) F_n(y), F_m(x) F_n^{(6)}(y)\} F_m(x) F_n(y) dx dy \tag{40}$$

$$\{\Lambda_{2400}, \Lambda_{4200}, \Lambda_{2600}\} = \int_0^a \int_0^b \{F_m^{(2)}(x) F_n^{(4)}(y), F_m^{(4)}(x) F_n^{(2)}(y), F_m^{(2)}(x) F_n^{(6)}(y)\} F_m(x) F_n(y) dx dy \tag{41}$$

$$\{\Lambda_{6200}, \Lambda_{8000}, \Lambda_{0800}\} = \int_0^a \int_0^b \{F_m^{(6)}(x)F_n^{(2)}(y), F_m^{(8)}(x)F_n(y), F_m(x)F_n^{(8)}(y)\} F_m(x)F_n(y) dx dy \quad (42)$$

For introduced conditions,  $F_m$  might be expressed as

$$\begin{aligned} F_m(x) &= \text{Sin}\left(\frac{m\pi}{a}x\right) \text{ for } SS \\ F_m(x) &= \text{Sin}^2\left(\frac{m\pi}{a}x\right) \text{ for } CC \end{aligned} \quad (43)$$

It is possible to derive  $F_n$  by replacing  $a, x, m$  with  $b, y, n$ .

By introducing mass matrix (M), stiffness matrix (K) and geometric matrix (G), the governing equation of nano-dimension plate exposed to time-dependent loads might be defined as

$$[M]\{\ddot{W}_{mn}\} + [[K] + N_0(t)[G]]\{W_{mn}\} = 0 \quad (44)$$

The time-dependent forced will be defined as  $N_0(t) = -[\alpha + \beta \cos(\varpi t)]N_{cr}$  based on static and dynamic load parameters ( $\alpha, \beta$ ) and critical buckling load ( $N_{cr}$ ); so above equation becomes

$$[M]\{\ddot{W}_{mn}\} + [[K] - \{\alpha + \beta \cos(\varpi t)\}N_{cr}[G]]\{W_{mn}\} = 0 \quad (45)$$

Here  $\varpi$  is the frequency of excitation for the time-dependent force and is normalized as

$$\Omega = \varpi h \sqrt{\frac{\rho_c}{E_c}} \quad (46)$$

The solution for such time-dependent problem based on Mathieu–Hill equation will be presented as follows

$$[[K] - N_{cr}\{\alpha \pm 0.5\beta\}[G] - 0.25\varpi[M]]\{W_{mn}\} = 0 \quad (47)$$

The solution of above equation is

$$\det \begin{vmatrix} [\bar{K}] - (0.5\beta)N_{cr}[G] - (0.25\varpi)[M] & 0 \\ 0 & [\bar{K}] + (0.5\beta)N_{cr}[G] - (0.25\varpi)[M] \end{vmatrix} = 0 \quad (48)$$

where  $[\bar{K}] = [K] - \alpha N_{cr}[G]$  and normalized coefficients are

$$K_w = \frac{k_w a^4}{D_c}, K_p = \frac{k_p a^2}{D_c}, D_c = \frac{E_c h^3}{12(1-\nu_c^2)} \quad (49)$$

#### 4. Results and discussions

Using 3-unknown plate theory, dynamic stability of nano-scale plates made of metal foam

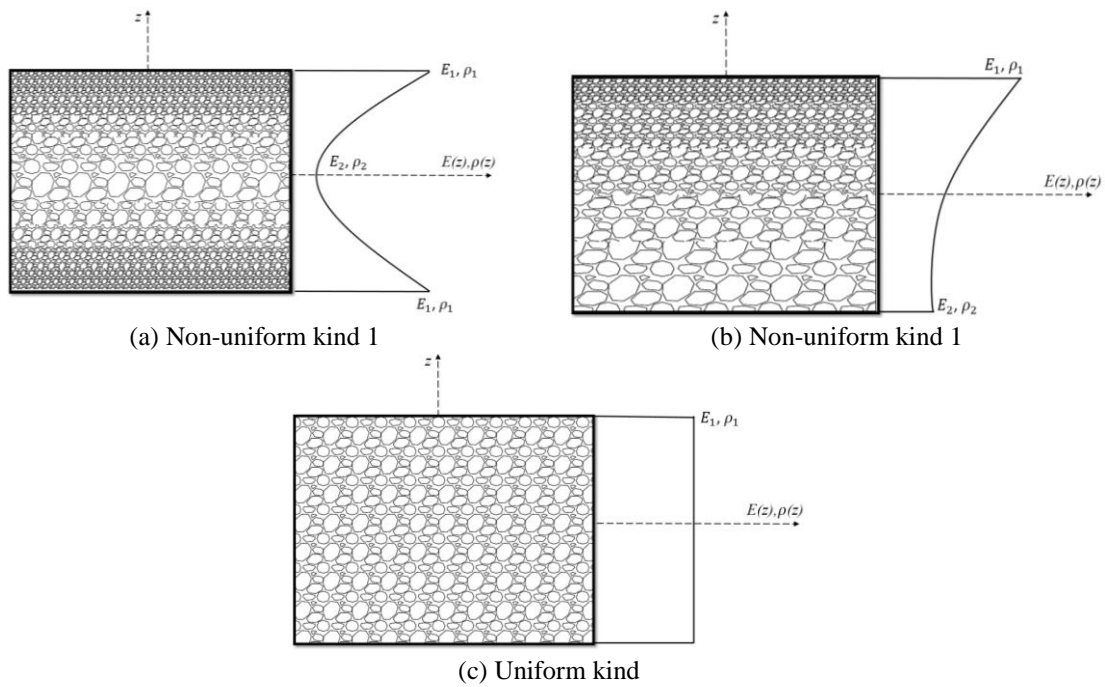


Fig. 1 Assumed pore variations in the plate

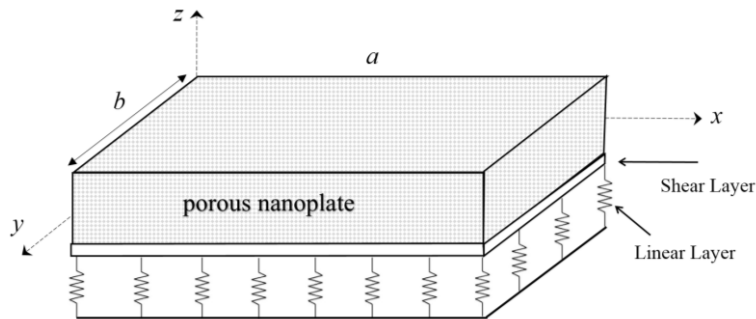


Fig. 2 Geometry and coordinates of porous nanoplate

subjected to in-plane periodic loads will be studied in this section. The material is steel be different pore distributions inside it. Nonlocal effects due to nano-dimension of the plate have been considered. The governing equations of the nano-dimension plate were solved with the help of Galerkin’s approach. The obtained stability regions due to applied periodic loads will be verified with the work of Han *et al.* 2015 and also the natural frequencies of a nanoplate will be verified by the work of Natarajan *et al.* 2012. These verifications are presented in Tables 1 and 2. The dynamic stability of metal foam nano-size plate is shown to be dependent on applied load factors, pore distribution, non-local impacts, and some other parameters. Herein, the material properties of steel foam plate will be selected as

- $E_1 = 200 \text{ GPa}, \rho_1 = 7850 \text{ kg/m}^3, \nu = 0.33,$

Table 1 Normalized frequency verification based on various factors at n=5

a/h	Fully simply-supported				Fully clamped			
	a=b		a=2b		a=b		a=2b	
	Natarajan <i>et al.</i> (2012)	present						
10	0.0441	0.043823	0.1055	0.104329	0.0758	0.078893	0.1789	0.189380
	0.0403	0.04007	0.0863	0.085493	0.0682	0.070135	0.1426	0.146338
	0.0374	0.037141	0.0748	0.074174	0.0624	0.063767	0.1218	0.123547
	0.0330	0.032806	0.0612	0.060673	0.0542	0.054949	0.0978	0.098461
20	0.0113	0.011256	0.0279	0.027756	0.0207	0.020954	0.0534	0.054706
	0.0103	0.010288	0.0229	0.022722	0.0186	0.018639	0.0422	0.042393
	0.0096	0.009534	0.0198	0.019704	0.0170	0.016953	0.0358	0.035836
	0.0085	0.008418	0.0162	0.016110	0.0147	0.014615	0.0287	0.028592

Table 2 Frequency verification of a plate under time-dependent forces at  $\beta=0.5$

		$\alpha=0$		$\alpha=0.1$		$\alpha=0.2$		$\alpha=0.3$	
		Han <i>et al.</i> (2015)	This article	Han <i>et al.</i> (2015)	This article	Han <i>et al.</i> (2015)	This article	Han <i>et al.</i> (2015)	This article
		$[\bar{K}] - (0.5\beta)N_{cr}[G]$	n=0.1	3.0113	3.01141	2.8033	2.80349	2.5787	2.57885
	n=1	2.9785	2.97861	2.7729	2.77295	2.5507	2.55075	2.3072	2.30725
	n=10	2.9365	2.93662	2.7337	2.73384	2.5147	2.51477	2.2746	2.2747
$[\bar{K}] + (0.5\beta)N_{cr}[G]$	n=0.1	3.8874	3.88761	3.7287	3.72889	3.5629	3.56309	3.389	3.3892
	n=1	3.8452	3.84531	3.6882	3.68830	3.5242	3.52431	3.3522	3.3523
	n=10	3.7910	3.79113	3.6362	3.63633	3.4745	3.47464	3.3049	3.30504

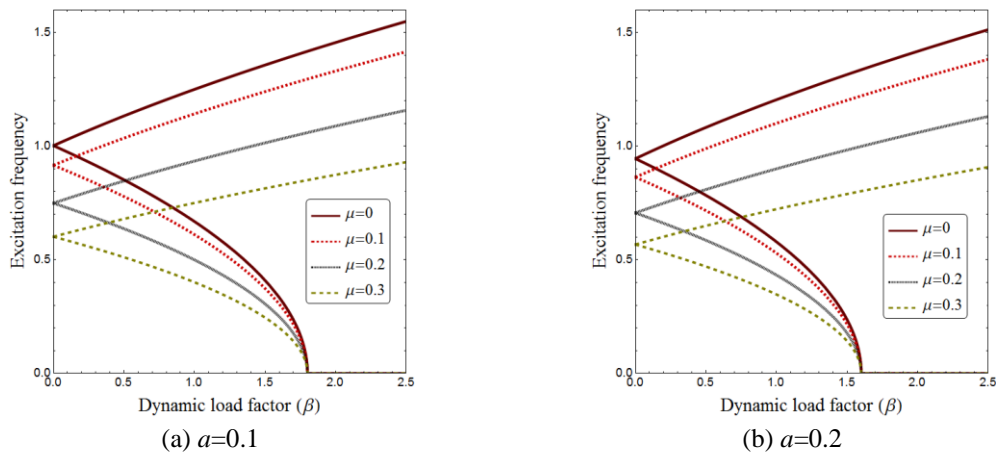
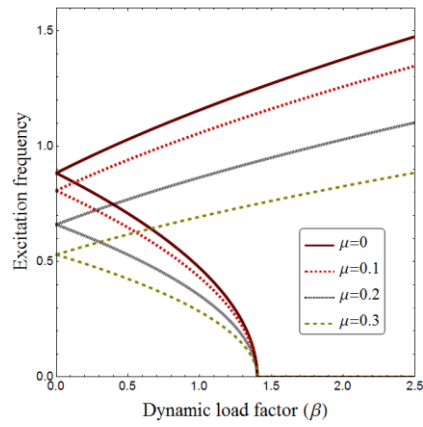
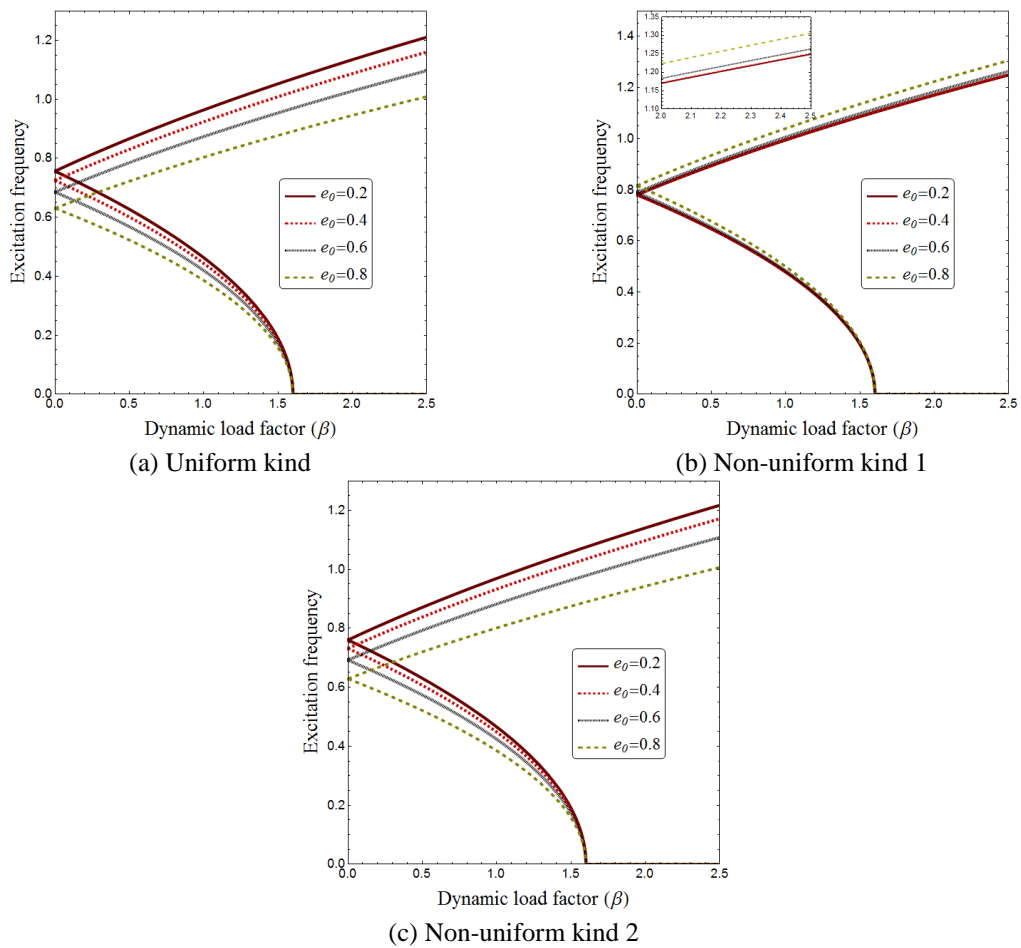


Fig. 3 Normalized frequency of nano-dimension plates with uniform porosities with respect to dynamical force coefficient for different non-local and static force coefficients ( $K_w=0, K_p=0, e_0=0.5, a/h=10$ )



(c)  $a=0.3$

Fig. 3 Continued



(a) Uniform kind

(b) Non-uniform kind 1

(c) Non-uniform kind 2

Fig. 4 Normalized frequency of nano-dimension plates versus dynamical force coefficient for different porosity distributions ( $\alpha=0.2$ ,  $K_w=0$ ,  $K_p=0$ ,  $\mu=0.2$ ,  $a/h=10$ )

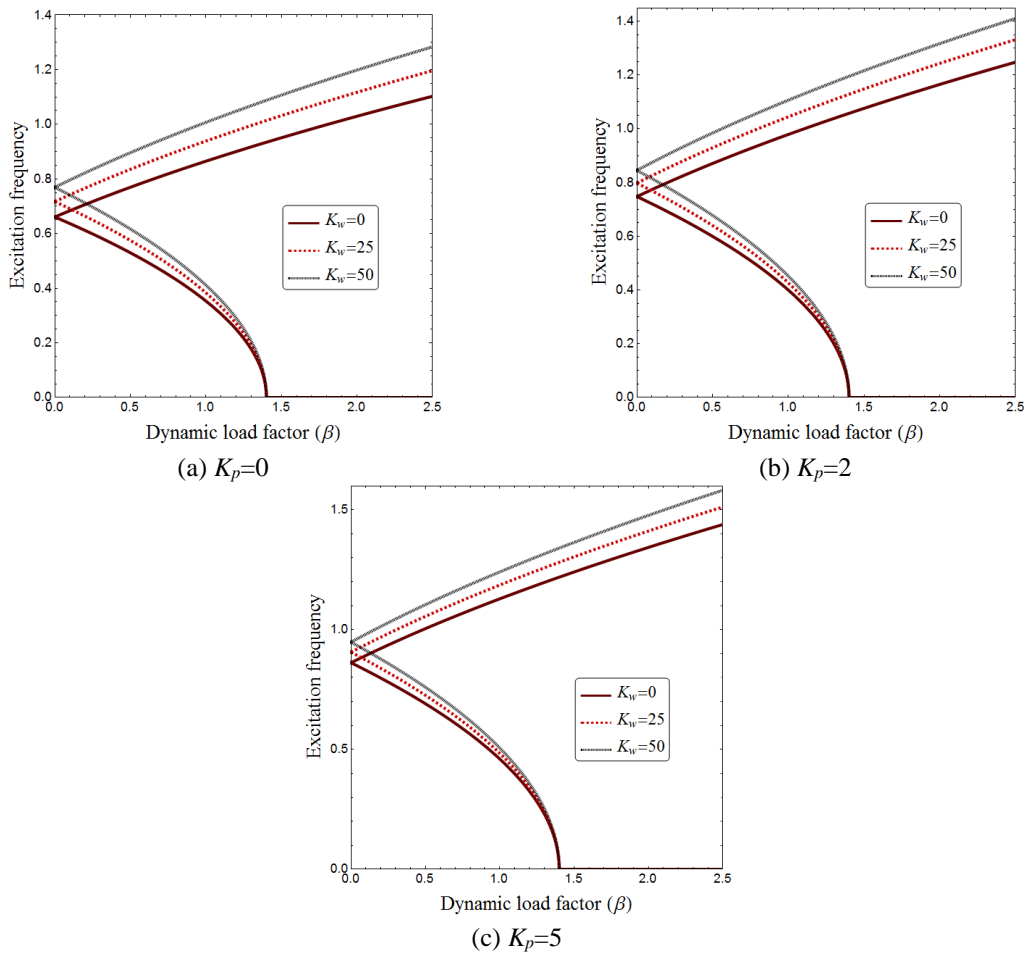


Fig. 5 Normalized frequency of nano-dimension plates versus dynamical force coefficient based on different foundation constants and uniform pores ( $a/h=10, \alpha=0.3, \mu=0.2, e_0=0.5$ )

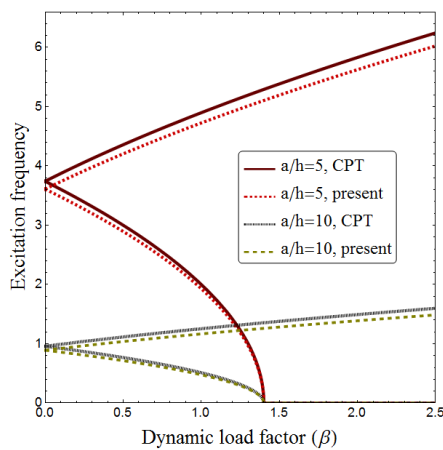


Fig. 6 Normalized frequency of nano-dimension plates versus dynamical force coefficient according to the classical and present plate theories ( $\alpha=0.3, \mu=0.2, K_w=50, K_p=5, e_0=0.5$ )

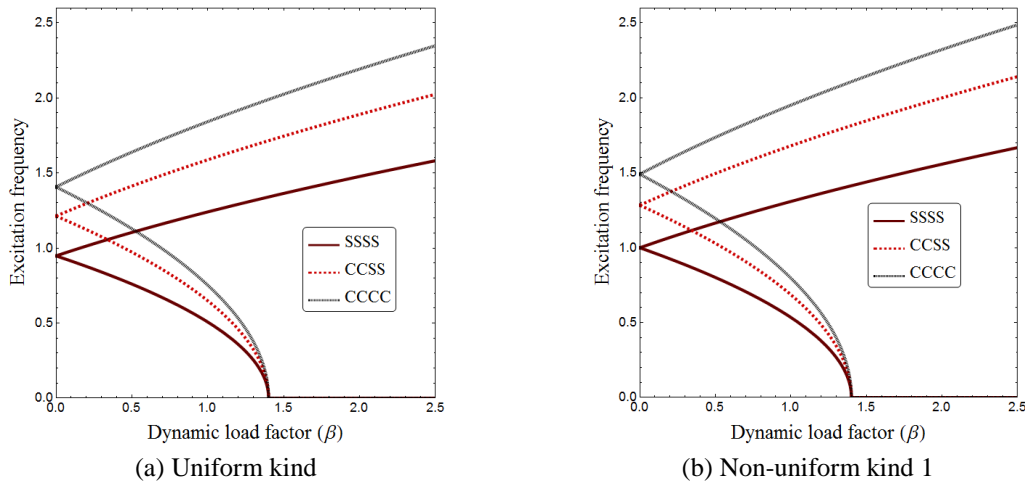


Fig. 7 Normalized frequency of nano-dimension plates versus dynamical force coefficient for different edge conditions ( $a/h=10$ ,  $\alpha=0.3$ ,  $\mu=0.2$ ,  $K_w=50$ ,  $K_p=5$ ,  $e_0=0.5$ )

Fig. 3 indicates the impact of static force coefficient ( $\alpha$ ) and non-local coefficient ( $\mu$ ) on dynamic buckling properties of nano-dimension porous plates when  $a/h=10$ ,  $e_0=0.5$  and  $K_w=K_p=0$ . One could observe that by the increment of non-local coefficient, the boundary of dynamic stability will be decreased. Actually, non-local effect will enhance the instability of the plate under time-dependent forces. Also, the value  $\beta=0$  denote the static buckling of the non-local plate and the obtained buckling load is called critical load for this situation. So, the critical load will be decreased with the growth of non-local coefficient (reduction in plate stiffness). This important fact makes the static/dynamic buckling of a nano-dimension plate different from a macro-dimension one. Another observation from the figure is that by the static force coefficient increment, the boundary of dynamic stability zone will be reduced at a prescribed non-local coefficient.

Pore content effects on instability boundary of a porous nanoplate with respect to dynamical force coefficient has been depicted in Fig. 4 at  $\mu=0.2$ ,  $\alpha=0.2$ ,  $K_w=0$  and  $K_p=0$ . An increase in porosity coefficient yields larger frequencies for nanoplates containing pore distribution 1 while smaller frequencies for nanoplates containing uniform porosities and dispersion 2. Obtained results indicate that by increase of the pore parameter, the nanoplate containing pore distribution 1 gives the greatest excitation frequencies while the results for a nanoplate containing uniform pores and graded pore dispersion 2 are relatively closer.

In Fig. 5, normalized excitation frequency variation according to dynamical forced coefficient ( $\beta$ ) based on different elastic foundation constants has been studied for simple-supported nanoplates when  $a/h=10$ ,  $\alpha=0.3$ ,  $\mu=0.2$ ,  $e_0=0.5$ . It is observable that increasing the foundation constants leads to greater normalized excitation frequencies. Actually, by increasing in foundation constants, the dynamic buckling boundaries will be shifted to higher values and excitation frequencies will grow.

Fig.6 shows the normalized excitation frequency variation of the porous nano-dimension plates according to dynamical force coefficient and classical and 3-unknown plate theories when  $\alpha=0.3$ ,  $\mu=0.2$ ,  $K_w=50$ ,  $K_p=5$ ,  $e_0=0.5$ . At a fixed dynamic load factor, it can be seen that frequency results according to the classical plate theory are overestimated. In fact, more accurate examination of

stability boundaries of porous nanoplates can be carried out employing higher order shear deformation plate theories. However, the value of side-to-thickness ratio has a remarkable influence on the instability boundaries. One can see that the width of instability boundaries for  $a/h=10$  is smaller than that of  $a/h=5$ . In other words, excitation frequency reduces with the increase of side-to-thickness ratio at a constant dynamic load factor.

Normalized excitation frequency variation according to dynamical force coefficient ( $\beta$ ) based on different edge condition (SSSS, CCSS and CCCC) at  $\alpha=0.3$ ,  $K_w=50$ ,  $K_p=5$  and  $\mu=0.2$  has been illustrated in Fig. 7. By assuming a prescribed dynamical force coefficient, the porous nano-dimension plate possessing harder edge condition gives greater normalized excitation frequencies. Thus, fully clamped boundary type exhibits greatest excitation frequencies followed by CCSS and SSSS. Therefore, the broadest stability zone might be derived based on fully clamped edge supports.

## 5. Conclusions

Using 3-unknown plate theory, dynamic stability of nano-scale plates made of metal foam subjected to in-plane periodic loads was studied in this paper. The material was steel with different pore distributions inside it. Nonlocal effects due to nano-dimension of the plate were considered. The governing equations of the nano-dimension plate were solved with the help of Galerkin's approach. The obtained stability regions due to applied periodic loads were verified with a previous work. The dynamic stability of metal foam nano-size plate was shown to be dependent on applied load factors, pore distribution, non-local impacts, and some other parameters. Non-local effect will enhance the instability of the plate under time-dependent forces. Also, by the static force coefficient increment, the boundary of dynamic stability zone will be reduced at a prescribed non-local coefficient.

## Acknowledgments

The researchers extend their thanks and appreciation to Mustansiriyah University and the College of Engineering.

## References

- Atmane, H.A., Tounsi, A. and Bernard, F. (2015a), "Effect of thickness stretching and porosity on mechanical response of a functionally graded beams resting on elastic foundations", *Int. J. Mech. Mater. Des.*, **13**(1), 1-14. <https://doi.org/10.1007/s10999-015-9318-x>.
- Atmane, H.A., Tounsi, A., Bernard, F. and Mahmoud, S.R. (2015b), "A computational shear displacement model for vibrational analysis of functionally graded beams with porosities", *Steel Compos. Struct.*, **19**(2), 369-384. <https://doi.org/10.12989/scs.2015.19.2.369>.
- Barati, M.R., Zenkour, A.M. and Shahverdi, H. (2016), "Thermo-mechanical buckling analysis of embedded nanosize FG plates in thermal environments via an inverse cotangential theory", *Compos. Struct.*, **141**, 203-212. <https://doi.org/10.1016/j.compstruct.2016.01.056>.
- Barati, M.R. and Zenkour, A.M. (2016), "Electro-thermoelastic vibration of plates made of porous functionally graded piezoelectric materials under various boundary conditions", *J. Vib. Control*, **24**(10), 1910-1926. <https://doi.org/10.1177/1077546316672788>.

- Barati, M.R. (2017a), "Nonlocal-strain gradient forced vibration analysis of metal foam nanoplates with uniform and graded porosities", *Adv. Nano Res.*, **5**(4), 393-414. <https://doi.org/10.12989/anr.2017.5.4.393>.
- Barati, M.R. (2017b), "Vibration analysis of FG nanoplates with nanovoids on viscoelastic substrate under hygro-thermo-mechanical loading using nonlocal strain gradient theory", *Struct. Eng. Mech.*, **64**(6), 683-693. <https://doi.org/10.12989/sem.2017.64.6.683>.
- Belabed, Z., Bousahla, A.A., Houari, M.S.A., Tounsi, A. and Mahmoud, S.R. (2018), "A new 3-unknown hyperbolic shear deformation theory for vibration of functionally graded sandwich plate", *Earthq. Struct.*, **14**(2), 103-115. <https://doi.org/10.12989/eas.2018.14.2.103>.
- Belkorissat, I., Houari, M.S.A., Tounsi, A., Bedia, E.A. and Mahmoud, S.R. (2015), "On vibration properties of functionally graded nano-plate using a new nonlocal refined four variable model", *Steel Compos. Struct.*, **18**(4), 1063-1081. <https://doi.org/10.12989/scs.2015.18.4.1063>.
- Bounouara, F., Benrahou, K.H., Belkorissat, I. and Tounsi, A. (2016), "A nonlocal zeroth-order shear deformation theory for free vibration of functionally graded nanoscale plates resting on elastic foundation", *Steel Compos. Struct.*, **20**(2), 227-249. <https://doi.org/10.12989/scs.2016.20.2.227>.
- Chen, D., Yang, J. and Kitipornchai, S. (2015), "Elastic buckling and static bending of shear deformable functionally graded porous beam", *Compos. Struct.*, **133**, 54-61. <https://doi.org/10.1016/j.compstruct.2015.07.052>.
- Chen, D., Yang, J. and Kitipornchai, S. (2016), "Free and forced vibrations of shear deformable functionally graded porous beams", *Int. J. Mech. Sci.*, **108**, 14-22. <https://doi.org/10.1016/j.ijmecsci.2016.01.025>.
- Ebrahimi, F. and Haghi, P. (2018), "A nonlocal strain gradient theory for scale-dependent wave dispersion analysis of rotating nanobeams considering physical field effects", *Coupled Syst. Mech.*, **7**(4), 373-393. <https://doi.org/10.12989/csm.2018.7.4.373>.
- Ebrahimi, F. and Daman, M. (2016), "Dynamic modeling of embedded curved nanobeams incorporating surface effects", *Coupled Syst. Mech.*, **5**(3), 255-268. <https://doi.org/10.12989/csm.2016.5.3.255>.
- Ebrahimi, F. and Heidari, E. (2018), "Surface effects on nonlinear vibration and buckling analysis of embedded FG nanoplates via refined HOSDPT in hygrothermal environment considering physical neutral surface position", *Adv. Aircraft Spacecraft Sci.*, **5**(6), 691-729. <https://doi.org/10.12989/aas.2018.5.6.691>.
- Ebrahimi, F., Babaei, R. and Shaghghi, G.R. (2018), "Nonlocal buckling characteristics of heterogeneous plates subjected to various loadings", *Adv. Aircraft Spacecraft Sci.*, **5**(5), 515-531. <https://doi.org/10.12989/aas.2018.5.5.515>.
- Eringen, A.C. (1983), "On differential equations of nonlocal elasticity and solutions of screw dislocation and surface waves", *J. Appl. Phys.*, **54**(9), 4703-4710. <https://doi.org/10.1063/1.332803>.
- Han, S.C., Park, W.T. and Jung, W.Y. (2015), "A four-variable refined plate theory for dynamic stability analysis of S-FGM plates based on physical neutral surface", *Compos. Struct.*, **131**, 1081-1089. <https://doi.org/10.1016/j.compstruct.2015.06.025>.
- Houari, M.S.A., Tounsi, A., Bessaim, A. and Mahmoud, S.R. (2016), "A new simple three-unknown sinusoidal shear deformation theory for functionally graded plates", *Steel Compos. Struct.*, **22**(2), 257-276. <https://doi.org/10.12989/scs.2016.22.2.257>.
- Jabbari, M., Hashemiteheri, M., Mojahedin, A. and Eslami, M.R. (2014), "Thermal buckling analysis of functionally graded thin circular plate made of saturated porous materials", *J. Thermal Stress.*, **37**(2), 202-220. <https://doi.org/10.1080/01495739.2013.839768>.
- Mahmoudi, A., Benyoucef, S., Tounsi, A., Benachour, A. and Bedia, E.A.A. (2018), "On the effect of the micromechanical models on the free vibration of rectangular FGM plate resting on elastic foundation", *Earthq. Struct.*, **14**(2), 117-128. <https://doi.org/10.12989/eas.2018.14.2.117>.
- Mehala, T., Belabed, Z., Tounsi, A. and Beg, O.A. (2018), "Investigation of influence of homogenization models on stability and dynamics of FGM plates on elastic foundations", *Geomech. Eng.*, **16**(3), 257-271. <https://doi.org/10.12989/gae.2018.16.3.257>.
- Mechab, B., Mechab, I., Benaissa, S., Ameri, M. and Serier, B. (2016), "Probabilistic analysis of effect of the porosities in functionally graded material nanoplate resting on Winkler-Pasternak elastic foundations", *Appl. Math. Modell.*, **40**(2), 738-749. <https://doi.org/10.1016/j.apm.2015.09.093>.
- Mirjavadi, S.S., Afshari, B.M., Barati, M.R. and Hamouda, A.M.S. (2018), "Strain gradient based dynamic

- response analysis of heterogeneous cylindrical microshells with porosities under a moving load”, *Mater. Res. Exp.*, **6**(3), 035029.
- Mirjavadi, S.S., Forsat, M., Barati, M.R., Abdella, G.M., Hamouda, A.M.S., Afshari, B.M. and Rabby, S. (2018), “Post-buckling analysis of piezo-magnetic nanobeams with geometrical imperfection and different piezoelectric contents”, *Microsyst. Technol.*, 1-12. <https://doi.org/10.1007/s00542-018-4241-3>.
- Mirjavadi, S.S., Afshari, B.M., Barati, M.R. and Hamouda, A.M.S. (2019a), “Transient response of porous FG nanoplates subjected to various pulse loads based on nonlocal stress-strain gradient theory”, *Eur. J. Mech. A Solids*, **74**, 210-220. <https://doi.org/10.1016/j.euromechsol.2018.11.004>.
- Mirjavadi, S.S., Afshari, B.M., Barati, M.R. and Hamouda, A.M.S. (2019b), “Nonlinear free and forced vibrations of graphene nanoplatelet reinforced microbeams with geometrical imperfection”, *Microsyst. Technol.*, 1-14. <https://doi.org/10.1007/s00542-018-4277-4>.
- Natarajan, S., Chakraborty, S., Thangavel, M., Bordas, S. and Rabczuk, T. (2012), “Size-dependent free flexural vibration behavior of functionally graded nanoplates”, *Comput. Mater. Sci.*, **65**, 74-80. <https://doi.org/10.1016/j.commatsci.2012.06.031>.
- Rezaei, A.S. and Saidi, A.R. (2016), “Application of Carrera Unified Formulation to study the effect of porosity on natural frequencies of thick porous-cellular plates”, *Compos. Part B Eng.*, **91**, 361-370. <https://doi.org/10.1016/j.compositesb.2015.12.050>.
- Sadoun, M., Houari, M.S.A., Bakora, A., Tounsi, A., Mahmoud, S.R. and Alwabli, A.S. (2018), “Vibration analysis of thick orthotropic plates using quasi 3D sinusoidal shear deformation theory”, *Geomech. Eng.*, **16**(2), 141-150. <https://doi.org/10.12989/gae.2018.16.2.141>.
- Yahia, S.A., Atmane, H.A., Houari, M.S.A. and Tounsi, A. (2015), “Wave propagation in functionally graded plates with porosities using various higher-order shear deformation plate theories”, *Struct. Eng. Mech.*, **53**(6), 1143-1165. <https://doi.org/10.12989/sem.2015.53.6.1143>.
- Wattanasakulpong, N. and Ungbhakorn, V. (2014), “Linear and nonlinear vibration analysis of elastically restrained ends FGM beams with porosities”, *Aerosp. Sci. Technol.*, **32**(1), 111-120. <https://doi.org/10.1016/j.ast.2013.12.002>.
- Zenkour, A.M. (2009), “The refined sinusoidal theory for FGM plates on elastic foundations”, *Int. J. Mech. Sci.*, **51**(11), 869-880. <https://doi.org/10.1016/j.ijmecsci.2009.09.026>.
- Zenkour, A.M. (2016), “Nonlocal transient thermal analysis of a single-layered graphene sheet embedded in viscoelastic medium”, *Physica E Low-dimen. Syst. Nanostruct.*, **79**, 87-97. <https://doi.org/10.1016/j.physe.2015.12.003>.